Quantitative coronary plaque characteristics on coronary computed tomography angiography and their prognostic value in patients with chronic kidney disease

Ning-Lang Yuan[1], Wen-Hao Zhu[2], Wei-Hua Yin[1], Rui Zhu[3], Yun-Qiang An[1], Zhi-Hui Hou[1], Bin Lu[1]

[1]Department of Radiology, Fuwai Hospital, Peking Union Medical College & Chinese Academy of Medical Sciences, State Key Lab and National Center for Cardiovascular Diseases, Beijing, China; [2]Department of Structural Heart Disease, Fuwai Hospital, Peking Union Medical College & Chinese Academy of Medical Sciences, Beijing, China; [3]Department of Nephrology, Fuwai Hospital, National Center for Cardiovascular Diseases, Chinese Academy of Medical Sciences and Peking Union Medical College, Beijing, China

Contributions: (I) Conception and design: R Zhu, WH Yin, ZH Hou; (II) Administrative support: B Lu; (III) Provision of study materials or patients: NL Yuan; (IV) Collection and assembly of data: NL Yuan; (V) Data analysis and interpretation: NL Yuan, YQ An; (VI) Manuscript writing: All authors; (VII) Final approval of manuscript: All authors.

Correspondence to: Zhi-Hui Hou, MD; Bin Lu, MD. Department of Radiology, Fuwai Hospital, Peking Union Medical College & Chinese Academy of Medical Sciences, State Key Lab and National Center for Cardiovascular Diseases, #167 Bei-Li-Shi Street, Beijing 100037, China. Email: konglingyihui@126.com; blu@vip.sina.com.

Background: Chronic kidney disease (CKD) is associated with an increased risk of cardiovascular events. This study compared coronary plaque characteristics assessed by coronary computed tomography angiography (CCTA) between patients with and without CKD and evaluated their associations with major adverse cardiovascular events (MACE).

Methods: This secondary analysis of the multicenter CREATION-CHINA cohort included patients with suspected coronary artery disease who underwent CCTA during 2016–2020. CKD was defined as an estimated glomerular filtration rate <60 mL/min/1.73 m^2. Propensity score matching (1:3) used age, sex, hypertension, diabetes mellitus, smoking, family history of coronary artery disease, and hyperlipidemia. Quantitative plaque characteristics and perivascular fat attenuation index (FAI) were assessed. MACE comprised all-cause death, non-fatal myocardial infarction, stroke, or revascularization >90 days after CCTA. Cox models estimated hazard ratios (HRs) and 95% confidence intervals (CIs); analyses of CCTA-derived predictors were adjusted for age, body mass index, and hypertension. High plaque burden was defined as total plaque burden in the highest quartile.

Results: After matching, 2,267 patients were included (588 with CKD and 1,679 without CKD). During a median follow-up of 3.47 years (interquartile range, 2.36–4.10), MACE occurred in 30 patients with CKD (5.1%) and 52 without CKD (3.1%; P=0.035). Patients with CKD had higher median total plaque volume (39.90 *vs.* 0 mm^3), median total plaque burden (8.83% *vs.* 0%), and prevalence of high-risk plaque (9.35% *vs.* 4.35%; all P<0.001). Among patients with CKD, lipid plaque burden (adjusted HR =1.107, 95% CI: 1.006–1.218; P=0.038) and high FAI (adjusted HR =4.027, 95% CI: 2.329–6.960; P<0.001) were independently associated with MACE. Compared with patients without CKD and with low plaque burden, those with CKD and high plaque burden had a higher risk of MACE (adjusted HR =6.153, 95% CI: 2.937–12.890; P<0.001).

Conclusions: CKD was associated with greater coronary plaque burden and a higher incidence of MACE. Lipid plaque burden and high FAI were independently associated with MACE after adjustment for age, body mass index, and hypertension, supporting their potential role in cardiovascular risk assessment in patients with CKD.

Keywords: Chronic kidney disease (CKD); coronary computed tomography angiography (CCTA); quantitative plaque analysis; plaque burden; major adverse cardiovascular events (MACE)

Submitted Feb 15, 2026. Accepted for publication Sep 28, 2026. Published online Oct 21, 2026.
doi: 10.21037/qims-2026-1-0396
View this article at: https://dx.doi.org/10.21037/qims-2026-1-0396

Introduction

Coronary artery disease (CAD) remains one of the leading causes of mortality and morbidity worldwide, primarily resulting from coronary atherosclerosis, and contributing substantially to myocardial ischemia, angina pectoris, and major adverse cardiovascular events (MACE) (1,2). Despite advances in preventive strategies and interventional therapies, the global prevalence of CAD continues to rise, with an especially pronounced burden among patients with chronic kidney disease (CKD) (3,4).

CKD is a highly prevalent non-communicable chronic condition that affects more than 10% of the global population. Its prevalence is steadily increasing, driven by aging populations and the growing incidence of metabolic disorders such as hypertension and diabetes (5,6). A substantial body of evidence has demonstrated a positive association between CKD and both the risk and severity of CAD. Declining renal function has been associated with accelerated atherosclerosis through multiple mechanisms, including oxidative stress, chronic inflammation, abnormalities in calcium-phosphorus metabolism, and endothelial dysfunction (7). Previous studies have shown that reduced creatinine clearance is closely linked to the risk of CAD, and that patients with CKD have a higher prevalence of triple-vessel disease, coronary stenosis, and calcification compared to non-CKD individuals (8).

However, most existing studies examining the relationship between CKD and CAD are limited by single-center designs, small sample sizes, and heterogeneous diagnostic methods, which constrain the generalizability and clinical applicability of their findings (9,10). Furthermore, many investigations have focused primarily on the overall cardiovascular risk associated with CKD, with relatively few providing systematic imaging-based evaluations of coronary atherosclerotic phenotypes across varying degrees of renal function (11). Traditional cardiovascular assessment tools—such as electrocardiography, echocardiography, and invasive angiography—are limited in their ability to detect early atherosclerotic changes.

In recent years, noninvasive imaging modalities such as coronary artery calcification score (CACS) and coronary computed tomography angiography (CCTA) have been increasingly used for early detection and risk stratification of CAD (12,13). Beyond luminal stenosis assessment, CCTA enables comprehensive quantification of plaque burden and characterization of plaque composition, including high-risk features such as low-attenuation plaque and positive remodeling (14,15). In addition, the perivascular fat attenuation index (FAI), derived from CCTA, has been proposed as a noninvasive imaging biomarker reflecting coronary inflammation and plaque activity. Previous studies have demonstrated associations between both quantitative plaque characteristics and FAI and adverse cardiovascular outcomes. Emerging evidence suggests that FAI may provide incremental prognostic information beyond traditional anatomical assessment.

Despite these advances, few studies have systematically integrated quantitative plaque burden, Coronary Artery Disease-Reporting and Data System (CAD-RADS) classification, high-risk plaque features, and inflammatory imaging markers such as FAI within a unified analytical framework. In particular, data remain scarce regarding the combined assessment of anatomical plaque characteristics and perivascular inflammatory indices in CKD populations, who represent a uniquely high-risk and pathophysiologically distinct group.

Against this backdrop, the present study leveraged data from the CREATION-CHINA study, a prospective, multicenter cohort designed to evaluate noninvasive imaging-based early detection and risk

stratification of coronary atherosclerosis in China. We included patients with and without CKD who underwent CCTA and applied propensity score matching (PSM) to balance baseline characteristics. We sought to (I) comprehensively compare coronary plaque burden, CAD-RADS categories, high-risk plaque features, and perivascular FAI between CKD and non-CKD patients, and (II) evaluate their prognostic associations with mid-term MACE. We present this article in accordance with the STROBE reporting checklist (available at https://qims.amegroups.com/article/view/10.21037/qims-2026-1-0396/rc).

Methods

Patient population

This study was based on the CREATION-CHINA cohort (NCT03518437), which enrolled patients with suspected CAD who underwent CCTA at multiple outpatient centers across China between January 2016 and December 2020. The design and inclusion/exclusion criteria of the cohort have been previously published (16,17). The study was conducted in accordance with the Declaration of Helsinki and its subsequent amendments. Patients were eligible for inclusion if they: (I) underwent high-quality CCTA suitable for quantitative plaque analysis; and (II) had complete renal function data, enabling classification into either CKD or non-CKD groups.

Exclusion criteria included: (I) poor image quality with severe motion artifacts or blooming artifacts impairing plaque identification and quantification; (II) severe heart failure (New York Heart Association class III–IV); (III) incomplete follow-up data or missing outcome information.

Estimated glomerular filtration rate (eGFR) was calculated using the simplified Modification of Diet in Renal Disease (MDRD) formula: $eGFR = 186 \times [\text{serum creatinine (mg/dL)}]^{-1.154} \times [\text{age (years)}]^{-0.203} \times 0.742$ (if female) (18). CKD was defined as eGFR <60 mL/min/1.73 m^2 according to the Kidney Disease: Improving Global Outcomes (KDIGO) guidelines. All patients were categorized into the CKD group (eGFR <60 mL/min/1.73 m^2) or the non-CKD group (eGFR ≥60 mL/min/1.73 m^2) (19).

To reduce baseline differences, PSM was performed using age, sex, and traditional cardiovascular risk factors (hypertension, diabetes mellitus, smoking, family history of CAD, and hyperlipidemia) as covariates. CKD patients were matched to non-CKD patients at a ratio of 1:3 to construct a comparison cohort (*Figure 1*). After matching, a total of 2,267 patients were included in the final analysis, comprising 588 in the CKD group and 1,679 in the non-CKD group.

Renal function and cardiovascular risk factors

Renal function was evaluated using the simplified MDRD equation as noted above. Based on the eGFR value, patients were stratified into CKD (eGFR <60 mL/min/1.73 m^2) and non-CKD (eGFR ≥60 mL/min/1.73 m^2) groups.

Traditional cardiovascular risk factors included smoking, hypertension, hyperlipidemia, diabetes, and family history of CAD. Smoking was defined as any smoking history within one year prior to CCTA. Hypertension was defined as systolic blood pressure ≥140 mmHg and/or diastolic blood pressure ≥90 mmHg, or a previous diagnosis of hypertension. Hyperlipidemia was defined according to the National Cholesterol Education Program (NCEP) guidelines (20). Diabetes was defined as fasting glucose ≥126 mg/dL or postprandial glucose ≥200 mg/dL. A family history of CAD was defined as a history of myocardial infarction, revascularization, or sudden cardiac death in the father before age 55 years or mother before age 65 years. Coronary atherosclerotic plaque was defined as any plaque-like lesion identified within the vessel wall on CCTA.

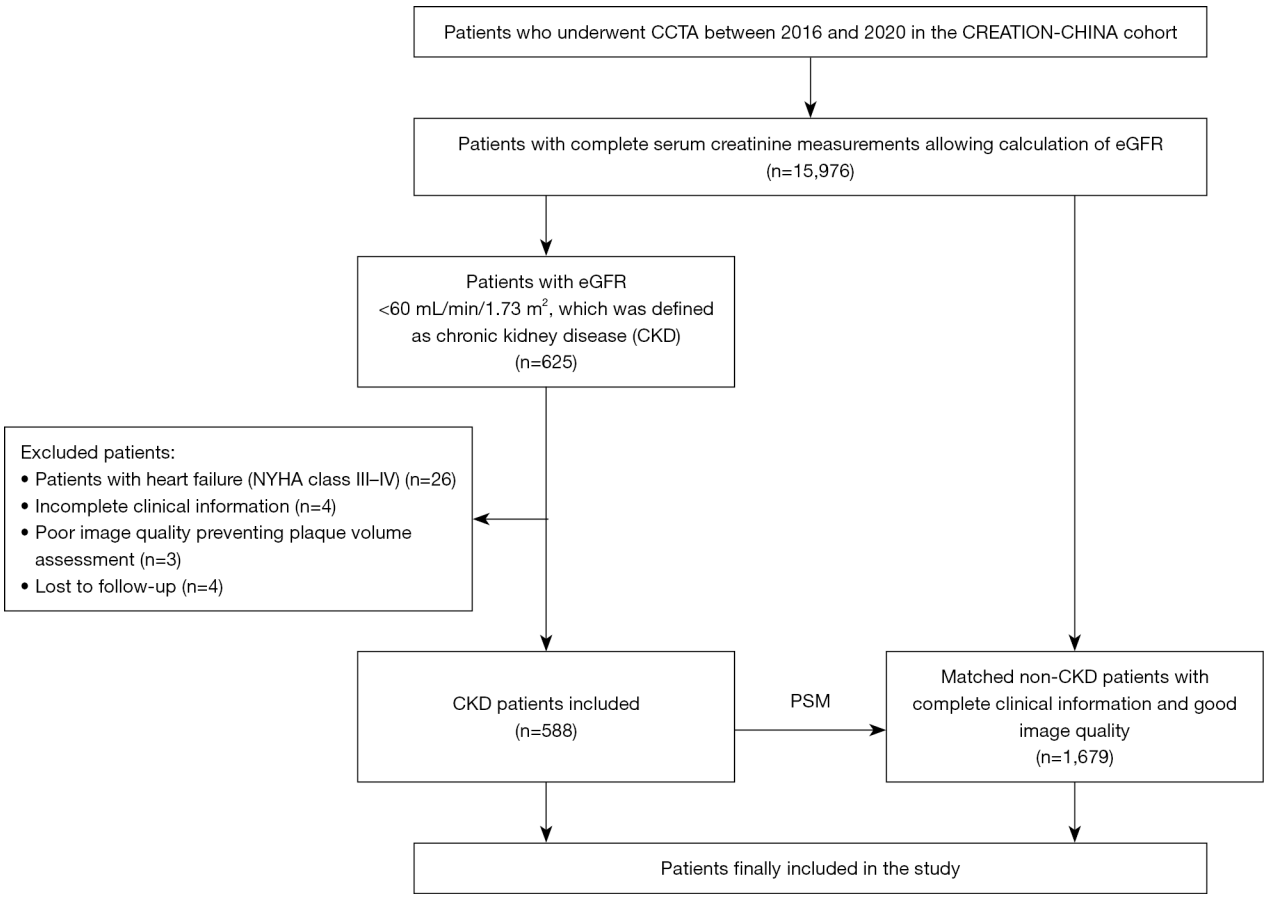


Figure 1 Study flowchart. PSM was performed using age, sex, and traditional cardiovascular risk factors—including hypertension, diabetes mellitus, smoking, family history of CAD, and hyperlipidemia—as covariates. CAD, coronary artery disease; CCTA, coronary computed tomography angiography; CKD, chronic kidney disease; eGFR, estimated glomerular filtration rate; NYHA, New York Heart Association; PSM, propensity score matching.

CCTA acquisition protocol

All CCTA examinations were performed using multidetector computed tomography (CT) scanners with at least 64 detector rows. Scanning parameters were adjusted based on body mass index (BMI): tube voltage was set to 100 kV for patients with BMI <30 kg/m^2 and to 120 kV for those with BMI ≥30 kg/m^2. Tube current was individually optimized according to BMI. A bolus-tracking technique was used to initiate contrast-enhanced scans, with a triggering threshold of 80–100 Hounsfield units (HU) and a scan delay of 6 seconds.

Key scanning parameters included a detector collimation of 0.5–0.6 mm, rotation time of 250–300 ms, pitch of 0.20–0.50, and a field of view (FOV) ranging from 180 to 250 mm to ensure high-resolution imaging. A three-phase contrast injection protocol was employed: (I) 50–60 mL of undiluted contrast agent (iopromide, 370 mg I/mL; Bayer Healthcare Inc., Berlin, Germany), followed by (II) 30 mL of contrast agent mixed with 70% saline, and (III) a 30 mL saline flush. All phases were injected at a rate of 4–5 mL/s. A non-contrast scan was performed prior to CCTA to evaluate coronary artery calcium score (CACS) using the Agatston method.

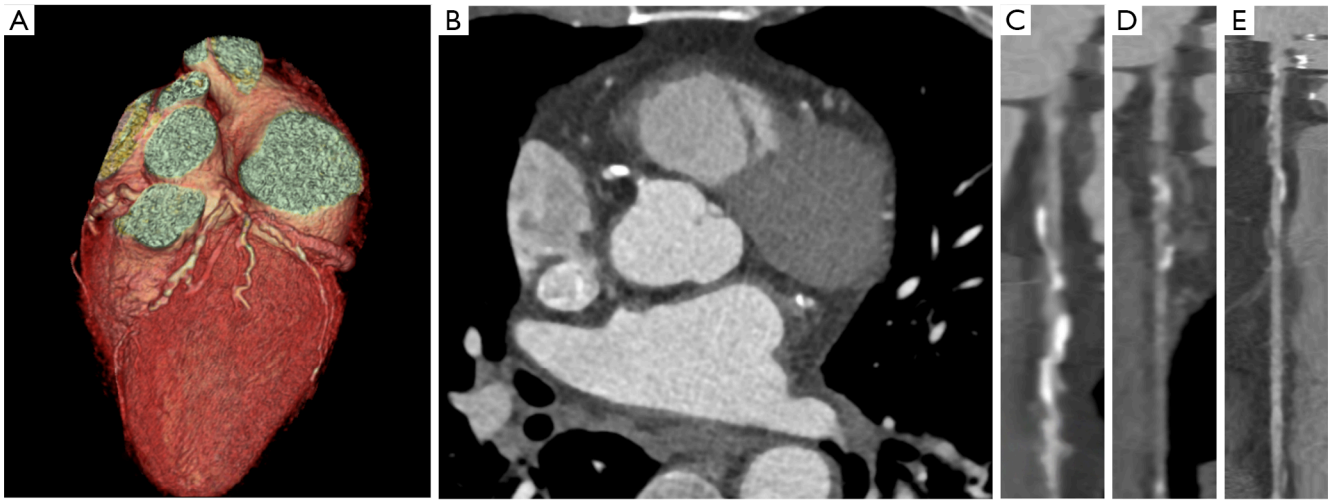


Figure 2 Representative case of coronary plaque. This case shows a 58-year-old patient with CKD. Volume-rendered (A) and cross-sectional (B) images demonstrate the distribution of coronary atherosclerotic plaques. Curved planar reformation images of the left anterior descending artery (C), left circumflex artery (D), and right coronary artery (E) reveal plaque involvement, indicating three-vessel disease. CKD, chronic kidney disease.

To improve coronary visualization and image quality, patients received sublingual glyceryl trinitrate (0.4–0.8 mg) before scanning. For patients with elevated heart rates, β-blockers were administered as clinically appropriate, aiming for a target heart rate below 65 beats per minute.

Concurrent use of nephrotoxic medications [e.g., nonsteroidal anti-inflammatory drugs (NSAIDs), aminoglycosides] was avoided. For patients with severe renal impairment (eGFR <30 mL/min/1.73 m^2) or those undergoing dialysis, individualized risk assessments were conducted, and scan timing was optimized —dialysis patients were preferably scanned prior to dialysis sessions.

All CCTA images were reconstructed using thin slices (0.5–0.75 mm) and post-processed with multiplanar reconstruction (MPR), maximum intensity projection (MIP), and volume rendering (VR) techniques to enable both qualitative and quantitative assessment of coronary artery anatomy and plaque characteristics. *Figure 2* presents representative CCTA images of a patient with CKD.

Image analysis and quantitative plaque assessment

All CCTA images were transferred to a centralized core laboratory for analysis. Plaque analysis was conducted on the ADW4.6 workstation (GE Healthcare, Milwaukee, WI, USA) using axial, multiplanar reformatted, and MIP images. Analyses were independently performed by two experienced radiologists, and discrepancies were resolved by a third senior radiologist. All image analyses were conducted blinded to clinical data and outcomes.

High-risk plaques were defined as those exhibiting ≥2 high-risk features on the same lesion, including: (I) spotty calcification: calcium deposit <3 mm in diameter. (II) Positive remodeling: remodeling index >1.1 (lesion diameter/reference diameter). (III) Low-attenuation plaque: CT attenuation <30 HU. (IV) Napkin-ring sign: low-density core surrounded by a higher-density rim (21). Coronary stenosis severity was assessed using the CAD-RADS: (I) CAD-RADS 0: no stenosis (0%). (II) CAD-RADS 1: minimal stenosis (1–24%). (III) CAD-RADS 2: mild stenosis (25–49%). (IV) CAD-RADS 3: moderate stenosis (50–69%). (V) CAD-RADS 4: severe stenosis (70–99%). (VI) CAD-RADS 5: total occlusion (100%)

(22). The most severe stenosis across all segments was used to represent patient-level stenosis severity. Obstructive CAD was defined as any segment with CAD-RADS grade 3–5. The number of diseased vessels referred to the count of coronary arteries with obstructive CAD among the major vessels left anterior descending artery (LAD), left circumflex artery (LCX), and right coronary artery (RCA), based on the American Heart Association 17-segment model. Left main disease was considered equivalent to two-vessel disease.

All images were reviewed by two radiologists with 8 and 10 years of experience in CCTA interpretation using a dedicated workstation (Deep Blue, ADW4.6; GE Healthcare). The coronary tree was automatically extracted and analyzed from the origin to the distal segments (<2.0 mm diameter) of the left main coronary artery (LM), LAD, LCX, and RCA arteries.

Lumen and vessel contours were automatically delineated and manually corrected when necessary. Cross-sectional verification was performed at 0.5-mm intervals. Attenuation values were calibrated using adaptive filtering to ensure consistency across datasets [8]. Plaque components were classified by HU thresholds: lipid-rich plaque (<30 HU), fibrous plaque (30–150 HU), and calcified plaque (>350 HU); luminal area was defined as 150–350 HU. A color overlay was applied to segment plaque components on the scan. Total plaque volume was calculated as the sum of the three components. Plaque burden (%) was quantified for total plaque, lipid-rich plaque, fibrous plaque, and calcified plaque using the following formula: plaque burden (%) = (plaque volume/vessel volume) × 100. The plaque burden of the entire coronary artery tree was defined as the average burden across all 17 segments, and the burden of individual plaque components (lipid-rich, fibrous, calcified) was similarly averaged per patient. Figure S1 shows examples of quantitative plaque measurements.

To evaluate measurement reproducibility, quantitative plaque analyses were independently repeated in a randomly selected subset of cases by a second experienced observer who was blinded to the original measurements. The same observer also repeated the analyses after an interval of at least 4 weeks. Interobserver and intraobserver agreement were assessed using intraclass correlation coefficients (ICCs).

In this study, the perivascular FAI was measured along the proximal segment of the LAD. The LAD was chosen because it is anatomically consistent, has a relatively straight course, and provides high-quality imaging with minimal motion artifacts, ensuring reproducible measurements. Previous studies have demonstrated that LAD-derived FAI is associated with coronary inflammation and cardiovascular outcomes, and may reflect global coronary inflammatory burden across the coronary tree (23,24). However, the optimal coronary segment for FAI assessment remains under investigation, and no universal consensus has been established. The proximal 40–50 mm of the LAD was selected for analysis, avoiding areas with heavy calcification or stents, and the perivascular adipose tissue immediately surrounding the vessel wall (approximately 1–3 mm radial distance) was segmented for HU-based attenuation measurement. Tissues with attenuation values ranging from −190 to −30 HU were defined as perivascular adipose tissue. The vessel centerline was automatically generated by the software, and the outer vessel contour was automatically identified after manual determination of the proximal and distal reference cross-sections of the target segment. Manual corrections were permitted when automatic detection was inaccurate.

Follow-up and clinical outcomes

All patients were followed for the occurrence of MACE, defined as a composite of all-cause death, non-fatal myocardial infarction (MI), stroke and late revascularization [defined as percutaneous coronary intervention (PCI) or coronary artery bypass grafting (CABG) performed >90 days after the index CCTA].

Follow-up was conducted through outpatient visits and structured telephone interviews by trained staff. For patients who experienced events or died, supporting clinical documentation (e.g., discharge

summaries, death certificates) was collected and adjudicated by an independent clinical events committee blinded to imaging findings.

Statistical analysis

To minimize baseline differences and potential confounding between patients with and without CKD, a PSM approach was employed. The propensity score was estimated using a logistic regression model that included age, sex, and traditional cardiovascular risk factors—hypertension, diabetes mellitus, smoking status, family history of CAD, and hyperlipidemia—as covariates. CKD patients were matched to non-CKD patients at a 1:3 ratio using a nearest-neighbor algorithm without replacement and a caliper width of 0.2 standard deviations of the logit of the propensity score. Covariate balance before and after matching was assessed using standardized mean differences (SMDs), with an SMD <0.1 considered indicative of adequate balance. As sensitivity analyses, inverse probability of treatment weighting (IPTW) and multivariable Cox regression analyses were performed in the full cohort. Propensity scores for IPTW were estimated using sex, age, BMI, obesity, hypertension, hyperlipidemia, diabetes mellitus, family history, and smoking status.

Continuous variables were evaluated for normality using the Shapiro-Wilk test. Normally distributed variables (age and body mass index) are presented as mean ± standard deviation (SD) and were compared using the Student's t-test. Non-normally distributed variables—including eGFR, laboratory biomarkers, follow-up duration, and quantitative plaque parameters—are expressed as median [interquartile range (IQR)] and were analyzed using the Mann-Whitney U test.

Categorical variables—including cardiovascular risk factors, vessel involvement categories, CAD-RADS classification, high-risk plaque characteristics, and clinical outcomes—are reported as frequencies and percentages and were compared using the Chi-squared test or Fisher's exact test, as appropriate.

Time-to-event analyses were conducted using Kaplan-Meier survival curves and the log-rank test. Cox proportional hazards regression models were applied to estimate hazard ratios (HRs) and 95% confidence intervals (CIs) for MACE, adjusting for potential confounding variables. High plaque burden was defined as total plaque burden within the highest quartile. Patients were then stratified into four subgroups based on CKD status and high plaque burden for subsequent Cox proportional hazards analyses.

All statistical analyses were conducted using R software (version 4.3.1; R Foundation for Statistical Computing, Vienna, Austria). A two-sided P value <0.05 was considered statistically significant.

Results

Study population and baseline characteristics

After 1:3 PSM, a total of 2,267 patients were included, comprising 588 CKD patients and 1,679 non-CKD patients. Some participants could not be matched due to non-overlapping propensity score distributions and were excluded from further analyses. As expected, eGFR was significantly lower in the CKD group than in the non-CKD group [median (IQR), 54.60 (49.67–57.50) *vs.* 87.73 (76.64–98.73) mL/min/1.73 m^2; P<0.001]. There were no significant differences in age, sex, BMI, hypertension, hyperlipidemia, diabetes, family history of CAD, or current smoking (all P>0.05).

CKD patients exhibited higher fasting glucose [5.70 (5.17–6.95) *vs.* 5.58 (5.13–6.43) mmol/L; P=0.014], lower high-density lipoprotein (HDL) cholesterol [1.17 (0.99–1.43) *vs.* 1.22 (1.02–1.43) mmol/L; P=0.027], and a trend toward higher low-density lipoprotein (LDL) cholesterol [2.54 (1.87–3.29) *vs.* 2.50 (1.95–3.03) mmol/L; P=0.094]. Renal function markers were markedly worse in CKD patients, including serum creatinine, blood urea nitrogen, and uric acid (all P<0.001). Inflammatory markers,

including high-sensitivity C-reactive protein (hs-CRP) and lipoprotein(a) [Lp(a)], were also elevated (P=0.004 and 0.040, respectively).

During a median follow-up of approximately 3.5 years, CKD patients had a higher incidence of MACE than non-CKD patients (5.1% *vs.* 3.1%; P=0.035), while Follow-up duration did not differ significantly between groups [median (IQR), 3.35 (2.38–4.08) *vs.* 3.53 (2.33–4.12] years, P=0.516). Details of demographic and clinical characteristics are shown in *Table 1*.

Table 1 Demographic and clinical characteristics of CKD and non-CKD groups

Variable	Overall (n=2,267)	CKD (n=588)	Non-CKD (n=1,679)	P value
Estimated eGFR (mL/min/1.73 m^2)	80.01 [59.64, 94.38]	54.60 [49.67, 57.50]	87.73 [76.64, 98.73]	<0.001
Age (years)	62.29±8.89	62.68±9.24	62.16±8.76	0.220
Male	922 (40.67)	234 (39.80)	688 (40.98)	0.651
Body mass index (kg/m^2)	25.48±3.29	25.34±3.19	25.53±3.33	0.217
Hypertension	1,423 (62.77)	371 (63.10)	1,052 (62.66)	0.889
Hyperlipidemia	515 (22.72)	137 (23.30)	378 (22.51)	0.738
Diabetes	592 (26.11)	158 (26.87)	434 (25.85)	0.666
Family history of CAD	827 (36.48)	197 (33.50)	630 (37.52)	0.091
Current smoker	541 (23.86)	138 (23.47)	403 (24.00)	0.838
Fasting glucose (mmol/L)	5.61 [5.14, 6.54]	5.70 [5.17, 6.95]	5.58 [5.13, 6.43]	0.014
Total cholesterol (mmol/L)	4.39 [3.70, 5.18]	4.36 [3.62, 5.18]	4.41 [3.72, 5.18]	0.200
Triglycerides (mmol/L)	1.51 [1.11, 2.10]	1.54 [1.10, 2.20]	1.50 [1.11, 2.07]	0.470
HDL cholesterol (mmol/L)	1.21 [1.01, 1.43]	1.17 [0.99, 1.43]	1.22 [1.02, 1.43]	0.027
LDL cholesterol (mmol/L)	2.50 [1.94, 3.12]	2.54 [1.87, 3.29]	2.50 [1.95, 3.03]	0.094
Serum creatinine (μmol/L)	77.00 [64.00, 94.00]	106.00 [94.00, 124.00]	69.70 [61.09, 80.00]	<0.001
Blood urea nitrogen (mmol/L)	5.54 [4.51, 6.70]	6.96 [5.69, 8.52]	5.12 [4.30, 6.20]	<0.001
Uric acid (μmol/L)	325.53 [270.00, 393.94]	388.00 [319.81, 457.35]	308.85 [259.52, 367.09]	<0.001
hs-CRP (mg/L)	1.37 [0.81, 1.98]	1.59 [0.67, 3.37]	1.36 [0.87, 1.83]	0.004
Lp(a) (mg/L)	121.08 [47.00, 281.25]	126.50 [50.88, 347.53]	116.73 [46.05, 269.68]	0.040
MACE events	82 (3.62)	30 (5.10)	52 (3.10)	0.035
Follow-up duration (years)	3.47 [2.36, 4.10]	3.35 [2.38, 4.08]	3.53 [2.33, 4.12]	0.516

Data are presented as mean ± standard deviation, n (%) or median [interquartile range]. Continuous variables were compared using the independent samples t-test or Mann-Whitney U test, and categorical variables were compared using the Chi-squared test. A P value <0.05 was considered statistically significant. CAD, coronary artery disease; CKD, chronic kidney disease; eGFR, estimated glomerular filtration rate; HDL, high-density lipoprotein; hs-CRP, high-sensitivity C-reactive protein; LDL, low-density lipoprotein; Lp(a), lipoprotein(a); MACE, major adverse cardiovascular events.

CCTA findings and quantitative plaque analysis

In terms of CCTA features, the CKD group exhibited more extensive coronary involvement and more severe stenosis as indicated by CAD-RADS scores. As shown in *Table 2*, CKD patients exhibited a markedly higher prevalence of multivessel involvement (P<0.001). Compared with non-CKD individuals, CKD patients exhibited a markedly lower proportion of normal coronary arteries and a significantly higher prevalence of single-, two-, and three-vessel disease (all P<0.001). High-risk plaque (HRP) features

on CCTA were more common in the CKD group across all assessed markers. Specifically, CKD patients showed higher rates of spotty calcification (13.95% *vs.* 9.71%, P=0.006), positive remodeling (12.24% *vs.* 5.60%, P<0.001), low-attenuation plaque (9.86% *vs.* 5.66%, P=0.001), and the napkin-ring sign (6.12% *vs.* 3.57%, P=0.012). Overall, the prevalence of high-risk plaque, defined as the presence of ≥2 high-risk plaque features within the same lesion, was significantly higher in the CKD group than in the non-CKD group (9.35% *vs.* 4.35%, P<0.001). FAI was significantly higher in CKD patients [median (IQR), −67.87 (−69.21 to −66.48) *vs.* −71.99 (−73.34 to −70.60); P<0.001], indicating increased coronary inflammation.

Table 2 Coronary CTA characteristics in CKD and non-CKD groups

Coronary CTA characteristic	Overall	Non-CKD group (n=1,679)	CKD group (n=588)	P value
Number of vessels involved				<0.001
0	1,850 (81.61)	1,497 (89.16)	353 (60.03)	
1	187 (8.25)	69 (4.11)	118 (20.07)	
2	109 (4.81)	43 (2.56)	66 (11.22)	
3	121 (5.34)	70 (4.17)	51 (8.67)	
CAD-RADS				<0.001
0	1,121 (49.45)	941 (56.05)	180 (30.61)	
1–2	729 (32.16)	556 (33.11)	173 (29.42)	
3–5	417 (18.39)	182 (10.84)	235 (39.97)	
High-risk plaque features				
Spotty calcification	245 (10.81)	163 (9.71)	82 (13.95)	0.006
Positive remodeling	166 (7.32)	94 (5.60)	72 (12.24)	<0.001
Low-attenuation plaque	153 (6.75)	95 (5.66)	58 (9.86)	0.001
Napkin-ring sign	96 (4.23)	60 (3.57)	36 (6.12)	0.012
High-risk plaque	128 (5.65)	73 (4.35)	55 (9.35)	<0.001
FAI	−71.20 [−72.86, −69.12]	−71.99 [−73.34, −70.60]	−67.87 [−69.21, −66.48]	<0.001

Data are presented as n (%) or median [interquartile range]. Categorical variables were compared using the Chi-squared test. P values <0.05 were considered statistically significant. CAD-RADS, Coronary Artery Disease-Reporting and Data System; CKD, chronic kidney disease; CTA, computed tomography angiography; FAI, perivascular fat attenuation index.

Quantitative plaque analysis (*Table 3*, *Figure 3*) showed that total plaque volume was significantly greater in CKD patients (median: 39.9 *vs.* 0 mm^3, P<0.001), indicating more extensive atherosclerosis. Subtype analysis revealed that the CKD group had significantly higher fibrous plaque volume (33.25 *vs.* 0 mm^3, P<0.001) and lipid-rich plaque volume (1.9 *vs.* 0 mm^3, P<0.001), while calcified plaque volume showed smaller yet statistically significant differences (P=0.037). In terms of standardized plaque burden, the CKD group showed significantly greater total plaque burden (median: 8.83% *vs.* 0%, P<0.001), fibrous plaque burden (8.05% *vs.* 0%, P<0.001), and lipid plaque burden (0.48% *vs.* 0%, P<0.001), indicating not only higher plaque volume but also higher proportions of vulnerable components. Calcified plaque burden was also statistically higher in CKD patients (P=0.028), though with relatively smaller differences.

Table 3 Quantitative analysis of plaque components and volumes in CKD and non-CKD patients

Plaque parameter/group	Minimum	25th percentile	Median	75th percentile	Maximum	P value
Total plaque volume (mm^3)						<0.001
Non-CKD patients	0	0	0	185.30	1,906.70	
CKD patients	0	0	39.90	227.60	2,309.00	
Calcified plaque volume (mm^3)						0.037
Non-CKD patients	0	0	0	0	230.20	
CKD patients	0	0	0	1.43	450.80	
Fibrous plaque volume (mm^3)						<0.001
Non-CKD patients	0	0	0	154.15	1,685.20	
CKD patients	0	0	33.25	189.58	1,769.60	
Lipid plaque volume (mm^3)						<0.001
Non-CKD patients	0	0	0	16.20	277.30	
CKD patients	0	0	1.90	23.23	369.00	
Total plaque burden (%)						<0.001
Non-CKD patients	0	0	0	20.81	69.25	
CKD patients	0	0	8.83	23.67	75.96	
Calcified plaque burden (%)						0.028
Non-CKD patients	0	0	0	0	18.54	
CKD patients	0	0	0	0.08	34.61	
Fibrous plaque burden (%)						<0.001
Non-CKD patients	0	0	0	17.56	54.64	
CKD patients	0	0	8.05	20.22	59.61	
Lipid plaque burden (%)						<0.001
Non-CKD patients	0	0	0	1.68	17.85	
CKD patients	0	0	0.48	2.27	20.75	

Comparisons between groups were performed using the Mann-Whitney U test. P values <0.05 were considered statistically significant. Plaque burden was calculated as plaque volume divided by vessel volume (%). CKD, chronic kidney disease.

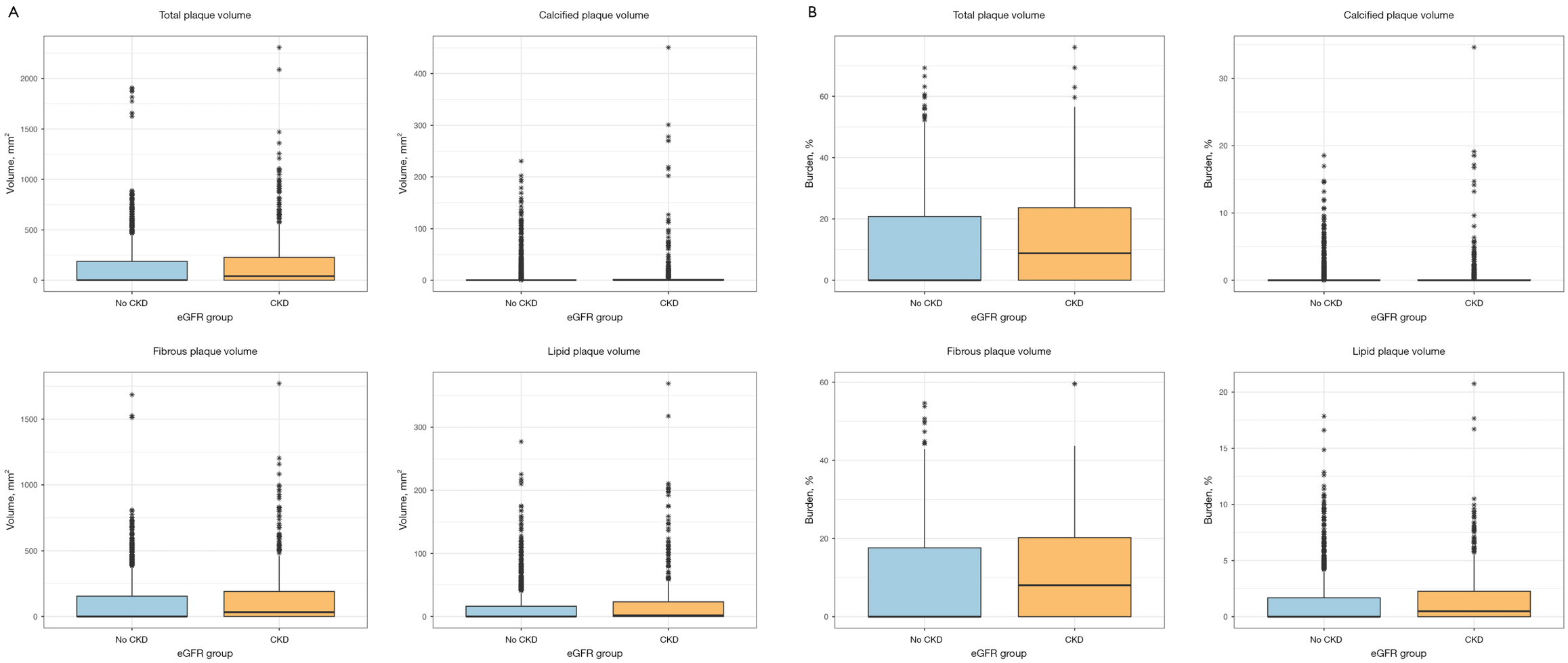


Figure 3 Comparison of plaque volume and burden between non-CKD and CKD groups. (A) Comparison of total, calcified, fibrous, and lipid plaque volumes between patients with CKD and those without. (B) Comparison of total, calcified, fibrous, and lipid plaque burdens between patients with CKD and those without. CKD, chronic kidney disease; eGFR, estimated glomerular filtration rate.

Reproducibility analyses demonstrated excellent agreement for quantitative plaque measurements. Interobserver ICCs ranged from 0.921 to 0.967, while intraobserver ICCs ranged from 0.980 to 0.989 (Table S1).

MACE and risk prediction

During a median follow-up of approximately 3.5 years, MACE occurred more frequently in the CKD group than in the non-CKD group (5.10% *vs.* 3.10%, P=0.035). Follow-up duration was similar between the two groups (*Table 1*, *Figure 4*). Cox regression analysis of clinical risk factors is presented in Table S2. Age, BMI, and hypertension were significantly associated with MACE and were therefore included as adjustment covariates in subsequent multivariable Cox regression analyses of CCTA-derived predictors. Cox proportional hazards regression was then performed to identify CCTA characteristics associated with MACE among CKD patients (*Table 4*). In CKD patients undergoing CCTA, several coronary CT characteristics were associated with MACE. Three-vessel disease and CAD-RADS category 3–5 were independently associated with a higher risk of MACE (multivariable HR =3.242, 95% CI: 1.825–5.762, P<0.001; HR =2.043, 95% CI: 1.322–3.158, P<0.001, respectively), whereas the absence of diseased vessels and CAD-RADS categories 0 and 1–2 were independently associated with a lower risk of MACE. Quantitative plaque analysis showed that high-risk plaque, total plaque volume, fibrous plaque volume, lipid plaque volume, and lipid plaque burden remained significant predictors of MACE after multivariable adjustment, with lipid plaque burden demonstrating an independent association with adverse cardiovascular events (HR =1.107, 95% CI: 1.006–1.218, P=0.038). In contrast, calcified plaque volume, total plaque burden, calcified plaque burden, and fibrous plaque burden were not independently associated with MACE. High FAI also remained an independent predictor of MACE (HR =4.027, 95% CI: 2.329–6.960, P<0.001). These results indicate that both the extent of CAD and plaque characteristics, particularly high-risk plaque, lipid-rich plaque, and increased perivascular inflammation, were independently associated with adverse cardiovascular outcomes in CKD patients after adjustment for age, BMI, and hypertension.

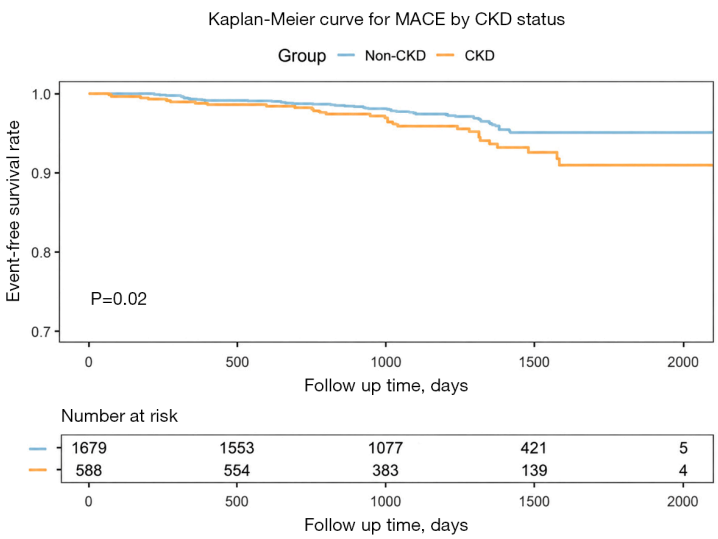


Figure 4 Comparison of Kaplan-Meier curves between non-CKD and CKD groups. Kaplan-Meier curves comparing survival free from MACE between patients with and without CKD. Differences between groups were assessed using the log-rank test (P=0.024). CKD, chronic kidney disease; MACE, major adverse cardiovascular events.

Table 4 Cox regression analysis of CCTA characteristics in CKD patients

CCTA characteristic	Univariable analysis		Multivariable analysis	
	HR (95% CI)	P	HR (95% CI)	P
Number of diseased vessels				
0	0.383 (0.169, 0.866)	0.021	0.489 (0.317, 0.756)	0.001
1	1.490 (0.804, 2.763)	0.205	1.314 (0.713, 2.423)	0.382
2	0.610 (0.217, 1.710)	0.348	1.230 (0.534, 2.833)	0.626
3	2.228 (1.137, 4.367)	0.020	3.242 (1.825, 5.762)	<0.001
CAD-RADS				
0	0.365 (0.153, 0.871)	0.023	0.109 (0.054, 0.220)	<0.001
1–2	0.617 (0.306, 1.242)	0.172	0.390 (0.255, 0.595)	<0.001
3–5	3.124 (1.674, 5.826)	<0.001	2.043 (1.322, 3.158)	<0.001
Quantitative analysis of plaque				
High-risk plaque	3.432 (1.682, 7.003)	<0.001	2.705 (1.151, 6.359)	0.023
Total plaque volume	1.001 (1.000, 1.002)	0.013	1.001 (1.000, 1.002)	0.015
Calcified plaque volume	1.002 (0.996, 1.009)	0.499	1.003 (0.997, 1.010)	0.322
Fibrous plaque volume	1.001 (1.000, 1.002)	0.014	1.001 (1.000, 1.003)	0.002
Lipid plaque volume	1.007 (1.003, 1.012)	0.002	1.008 (1.003, 1.013)	0.002
Total plaque burden	1.023 (1.003, 1.044)	0.027	1.020 (0.998, 1.043)	0.080
Calcified plaque burden	1.034 (0.947, 1.129)	0.457	1.046 (0.959, 1.141)	0.308
Fibrous plaque burden	1.025 (0.990, 1.052)	0.056	1.020 (0.992, 1.049)	0.157
Lipid plaque burden	1.135 (1.034, 1.245)	0.008	1.107 (1.006, 1.218)	0.038
FAI[†]	3.986 (1.629, 9.751)	0.002	4.027 (2.329, 6.960)	<0.001

[†], high FAI was defined as FAI score around the LAD ≥ the 50th percentile. CAD, coronary artery disease; CAD-RADS, Coronary Artery Disease-Reporting and Data System; CCTA, coronary computed tomography angiography; CI, confidence interval; CKD, chronic kidney disease; FAI, perivascular fat attenuation index; HR, hazard ratio; LAD, left anterior descending artery.

Joint effects of CKD and plaque burden on MACE risk

The joint association of CKD and plaque burden with the risk of MACE is presented in *Table 5*. The impact of CKD and plaque burden on MACE was assessed using Cox proportional hazards models. CKD alone was associated with an increased risk of MACE (univariable HR =1.671, 95% CI: 1.066–2.619, P=0.025; multivariable HR =2.271, 95% CI: 1.508–3.422, P<0.001), and high plaque burden alone was also independently associated with an increased risk of MACE (univariable HR =4.091, 95% CI: 2.650–6.316, P<0.001; multivariable HR =3.388, 95% CI: 2.229–5.151, P<0.001). Using patients without CKD and with low plaque burden as the reference group, CKD with low plaque burden was associated with a significantly higher risk of MACE (univariable HR =2.749, 95% CI: 1.478–5.113, P=0.001; multivariable HR =3.267, 95% CI: 1.683–6.340, P<0.001). Likewise, both non-CKD patients with high plaque burden (univariable HR =6.106, 95% CI: 3.504–10.639, P<0.001; multivariable HR =7.559, 95% CI: 4.229–13.512, P<0.001) and CKD patients with high plaque burden (univariable HR =5.283, 95% CI: 2.546–10.964, P<0.001; multivariable HR =6.153, 95% CI: 2.937–12.890, P<0.001) exhibited markedly increased risks of MACE. These findings suggest that both CKD and high plaque burden were independently associated with adverse cardiovascular outcomes, and that patients with both CKD and

high plaque burden also experienced a substantially increased risk of MACE after adjustment for age, BMI, and hypertension.

Table 5 Joint effects of chronic kidney disease and plaque burden on risk of MACE

Exposure/subgroup	N	MACE, n (%)	Univariable		Multivariable	
			HR (95% CI)	P value	HR (95% CI)	P value
Univariable associations						
CKD only	588	30 (5.10)	1.671 (1.066, 2.619)	0.025	2.271 (1.508, 3.422)	<0.001
High plaque burden only	567	47 (8.29)	4.091 (2.650, 6.316)	<0.001	3.388 (2.229, 5.151)	<0.001
Joint associations						
Non-CKD + low plaque burden	1, 274	17 (1.30)	Reference	Reference	Reference	Reference
CKD + low plaque burden	426	18 (4.20)	2.749 (1.478, 5.113)	0.001	3.267 (1.683, 6.340)	<0.001
Non-CKD + high plaque burden	405	35 (8.60)	6.106 (3.504, 10.639)	<0.001	7.559 (4.229, 13.512)	<0.001
CKD + high plaque burden	162	12 (7.40)	5.283 (2.546, 10.964)	<0.001	6.153 (2.937, 12.890)	<0.001

Multivariable models were adjusted for age, BMI, and hypertension. BMI, body mass index; CI, confidence interval; CKD, chronic kidney disease; HR, hazard ratio; MACE, major adverse cardiovascular events.

Sensitivity analyses

Sensitivity analyses using IPTW and multivariable Cox regression in the full cohort yielded generally consistent results with the primary analyses. Total plaque volume remained significantly associated with MACE in both analytical approaches, supporting the robustness of the primary findings (Table S3).

Discussion

In this multicenter, propensity score–matched CCTA cohort, our study extends previous evidence by demonstrating that patients with CKD exhibit a higher coronary plaque burden, more frequent high-risk plaque features, and greater non-calcified and lipid-rich plaque volumes compared with non-CKD individuals. Previous studies have shown associations between quantitative plaque characteristics, FAI, and adverse cardiovascular outcomes (25,26). In our study, these differences persisted despite comparable baseline cardiovascular risk factors and were associated with an increased incidence of mid-term MACE. Moreover, both quantitative plaque measures and FAI were independently associated with MACE after adjustment for conventional cardiovascular risk factors, supporting their potential value for risk stratification in patients with CKD.

These imaging findings are consistent with the known pathophysiological alterations in CKD. Metabolic dysregulation, chronic low-grade inflammation, oxidative stress, and endothelial dysfunction are all associated with accelerated atherosclerotic processes and may contribute to the development of more vulnerable plaque phenotypes. Such plaques, particularly non-calcified and mixed components, are considered more prone to instability and are associated with a higher likelihood of acute coronary events (27,28).

Consistent with prior studies, CKD has been recognized as an independent risk factor for coronary atherosclerosis and is associated with more extensive and complex plaque morphology. High-risk CCTA

features, including low-attenuation plaque, positive remodeling, and the napkin-ring sign, have been reported more frequently in CKD populations and are linked to adverse outcomes (29,30). In the PARADIGM substudy, CKD was associated with greater baseline plaque volume, whereas declining renal function was associated with more rapid plaque progression (31).

Compared with previous work, our study further integrates quantitative plaque assessment, CAD-RADS classification, and perivascular FAI within a multicenter cohort, providing a more comprehensive characterization of coronary atherosclerosis in CKD. Notably, even in stable outpatient populations, CKD was associated with increased non-calcified and lipid-rich plaque burden, suggesting that plaque composition and inflammatory activity may offer additional information beyond calcification-based assessment.

From a clinical perspective, these findings suggest that conventional risk assessment may underestimate cardiovascular risk in patients with CKD. Beyond coronary atherosclerosis, uremia-related cardiac remodeling and left ventricular diastolic dysfunction may also contribute to the overall cardiovascular burden in this population (32). Incorporating CCTA-derived quantitative plaque metrics and FAI may provide complementary information for cardiovascular risk assessment and characterization of coronary atherosclerotic burden in patients with CKD.

Several limitations should be acknowledged. First, although PSM was applied, residual confounding cannot be excluded due to the observational study design. Second, CKD was defined based on a single baseline eGFR measurement, without systematic assessment of kidney damage markers such as albuminuria. Third, the number of outcome events was relatively limited, which may affect the robustness of subgroup analyses. Fourth, medication data were not uniformly available and therefore were not incorporated into the analyses. In addition, inflammatory biomarkers and detailed measures of CKD severity (e.g., albuminuria or longitudinal renal function data) were not consistently available. These unavailable data may have contributed to residual confounding. Fifth, the composite endpoint included late revascularization. Restricting revascularization events to those occurring >90 days after the index CCTA was intended to reduce the influence of immediate management decisions triggered by baseline imaging findings. However, baseline CCTA findings and subsequent clinical assessment may still have influenced revascularization decisions during follow-up, potentially contributing to the observed association between CCTA characteristics and the composite endpoint. Therefore, treatment-referral bias and partial circularity cannot be completely excluded.

Conclusions

In conclusion, CKD is associated with a higher coronary plaque burden, more frequent high-risk plaque features, and increased perivascular inflammation on CCTA. These imaging features are independently associated with mid-term MACE. Quantitative plaque analysis and FAI were independently associated with adverse cardiovascular outcomes after adjustment for conventional cardiovascular risk factors and may provide complementary information for cardiovascular risk assessment in patients with CKD.

Acknowledgments

An abstract of this study was published in the supplement for the 21st Annual Scientific Meeting of the Society of Cardiovascular Computed Tomography (SCCT), 2026.

Footnote

Reporting Checklist: The authors have completed the STROBE reporting checklist. Available at https://qims.amegroups.com/article/view/10.21037/qims-2026-1-0396/rc

Funding: This work was supported by the Ministry of Science and Technology of China, National Key Research and Development Project (No. 2016YFC1300400).

Conflicts of Interest: All authors have completed the ICMJE uniform disclosure form (available at https://qims.amegroups.com/article/view/10.21037/qims-2026-1-0396/coif). All authors report support from the Ministry of Science and Technology of China, National Key Research and Development Project. The authors have no other conflicts of interest to declare.

Ethical Statement: The authors are accountable for all aspects of the work in ensuring that questions related to the accuracy or integrity of any part of the work are appropriately investigated and resolved. The study was conducted in accordance with the Declaration of Helsinki and its subsequent amendments.

Open Access Statement: This is an Open Access article distributed in accordance with the Creative Commons Attribution-NonCommercial-NoDerivs 4.0 International License (CC BY-NC-ND 4.0), which permits the non-commercial replication and distribution of the article with the strict proviso that no changes or edits are made and the original work is properly cited (including links to both the formal publication through the relevant DOI and the license). See: https://creativecommons.org/licenses/by-nc-nd/4.0/.

References

1. Jespersen L, Hvelplund A, Abildstrøm SZ, Pedersen F, Galatius S, Madsen JK, Jørgensen E, Kelbæk H, Prescott E. Stable angina pectoris with no obstructive coronary artery disease is associated with increased risks of major adverse cardiovascular events. Eur Heart J 2012;33:734-44.
2. Malakar AK, Choudhury D, Halder B, Paul P, Uddin A, Chakraborty S. A review on coronary artery disease, its risk factors, and therapeutics. J Cell Physiol 2019;234:16812-23.
3. KDIGO 2024 Clinical Practice Guideline for the Evaluation and Management of Chronic Kidney Disease. Kidney. Int 2024;105:S117-314.
4. Yiu KH, de Graaf FR, Schuijf JD, van Werkhoven JM, van Velzen JE, Boogers MJ, Roos CJ, de Bie MK, Pazhenkottil A, Kroft LJ, Boersma E, Herzog B, de Roos A, Kaufmann PA, Bax JJ, Jukema JW. Prognostic value of renal dysfunction for the prediction of outcome versus results of computed tomographic coronary angiography. Am J Cardiol 2011;108:968-72.
5. Sarnak MJ, Amann K, Bangalore S, Cavalcante JL, Charytan DM, Craig JC, Gill JS, Hlatky MA, Jardine AG, Landmesser U, Newby LK, Herzog CA, Cheung M, Wheeler DC, Winkelmayer WC, Marwick TH; Conference Participants. Chronic Kidney Disease and Coronary Artery Disease: JACC State-of-the-Art Review. J Am Coll Cardiol 2019;74:1823-38.
6. Fernández-Ruiz I. No benefit of initial invasive strategy for managing CAD in advanced CKD. Nat Rev Cardiol 2020;17:320-1.
7. Fang Z, Raza U, Song J, Lu J, Yao S, Liu X, Zhang W, Li S. Systemic aging fuels heart failure: Molecular mechanisms and therapeutic avenues. ESC Heart Fail 2025;12:1059-80.

8. Jug B, Kadakia J, Gupta M, Papazian J, Derakhshani A, Koplik S, Karlsberg RP, Budoff MJ. Coronary calcifications and plaque characteristics in patients with end-stage renal disease: a computed tomographic study. Coron Artery Dis 2013;24:501-8.
9. Deng W, Peng L, Yu J, Shuai T, Chen Z, Li Z. Characteristics of coronary artery atherosclerotic plaques in chronic kidney disease: evaluation with coronary CT angiography. Clin Radiol 2019;74:731.
10. Cheng XS, Mohanty S, Turner V, Mastrodicasa D, Winther S, Fleischmann D, Tan JC, Fearon WF. Coronary Computed Tomography Angiography in Diagnosing Obstructive Coronary Artery Disease in Patients with Advanced Chronic Kidney Disease: A Systematic Review and Meta-Analysis. Cardiorenal Med 2021;11:44-51.
11. Gruberg L, Rai P, Mintz GS, Canos D, Pinnow E, Satler LF, Pichard AD, Kent KM, Waksman R, Lindsay J, Weissman NJ. Impact of renal function on coronary plaque morphology and morphometry in patients with chronic renal insufficiency as determined by intravascular ultrasound volumetric analysis. Am J Cardiol 2005;96:892-6.
12. Han D, Klein E, Friedman J, Gransar H, Achenbach S, Al-Mallah MH, et al. Prognostic significance of subtle coronary calcification in patients with zero coronary artery calcium score: From the CONFIRM registry. Atherosclerosis 2020;309:33-8.
13. Nurmohamed NS, van Rosendael AR, Danad I, Ngo-Metzger Q, Taub PR, Ray KK, Figtree G, Bonaca MP, Hsia J, Rodriguez F, Sandhu AT, Nieman K, Earls JP, Hoffmann U, Bax JJ, Min JK, Maron DJ, Bhatt DL. Atherosclerosis evaluation and cardiovascular risk estimation using coronary computed tomography angiography. Eur Heart J 2024;45:1783-800. Erratum in: Eur Heart J. 2024 Jul 9;45(26):2332.
14. Nurmohamed NS, Bom MJ, Jukema RA, de Groot RJ, Driessen RS, van Diemen PA, de Winter RW, Gaillard EL, Sprengers RW, Stroes ESG, Min JK, Earls JP, Cardoso R, Blankstein R, Danad I, Choi AD, Knaapen P. AI-Guided Quantitative Plaque Staging Predicts Long-Term Cardiovascular Outcomes in Patients at Risk for Atherosclerotic CVD. JACC Cardiovasc Imaging 2024;17:269-80.
15. Chan K, Wahome E, Tsiachristas A, Antonopoulos AS, Patel P, Lyasheva M, et al. Inflammatory risk and cardiovascular events in patients without obstructive coronary artery disease: the ORFAN multicentre, longitudinal cohort study. Lancet 2024;403:2606-18.
16. Zheng J, Hou Z, Yin W, Gao Y, Ma Y, Lu B. Performance of the 2019 ESC pre-test probability model in predicting obstructive coronary artery disease in a Chinese population using coronary computed tomography angiography outcomes. J Cardiovasc Comput Tomogr 2024;18:408-15.
17. Zheng J, Hou Z, Gao Y, Yin W, Ma Y, An Y, Wang Y, Song L, Lu B. Coronary computed tomography angiography versus guideline-recommended clinical risk assessment for statin allocation in outpatients with suspected coronary artery disease. Am J Prev Cardiol 2025;22:100995.
18. Levey AS, Bosch JP, Lewis JB, Greene T, Rogers N, Roth D. A more accurate method to estimate glomerular filtration rate from serum creatinine: a new prediction equation. Modification of Diet in Renal Disease Study Group. Ann Intern Med 1999;130:461-70.
19. Levey AS, Eckardt KU, Tsukamoto Y, Levin A, Coresh J, Rossert J, De Zeeuw D, Hostetter TH, Lameire N, Eknoyan G. Definition and classification of chronic kidney disease: a position statement from Kidney Disease: Improving Global Outcomes (KDIGO). Kidney Int 2005;67:2089-100.
20. Expert Panel on Detection, Evaluation, and Treatment of High Blood Cholesterol in Adults. Executive Summary of The Third Report of The National Cholesterol Education Program (NCEP) Expert Panel on Detection, Evaluation, And Treatment of High Blood Cholesterol In Adults (Adult Treatment Panel III). JAMA 2001;285:2486-97.

21. Thomsen C, Abdulla J. Characteristics of high-risk coronary plaques identified by computed tomographic angiography and associated prognosis: a systematic review and meta-analysis. Eur Heart J Cardiovasc Imaging 2016;17:120-9.
22. Cury RC, Leipsic J, Abbara S, Achenbach S, Berman D, Bittencourt M, et al. CAD-RADS™ 2.0 - 2022 Coronary Artery Disease-Reporting and Data System: An Expert Consensus Document of the Society of Cardiovascular Computed Tomography (SCCT), the American College of Cardiology (ACC), the American College of Radiology (ACR), and the North America Society of Cardiovascular Imaging (NASCI). JACC Cardiovasc Imaging 2022;15:1974-2001.
23. Antonopoulos AS, Sanna F, Sabharwal N, Thomas S, Oikonomou EK, Herdman L, et al. Detecting human coronary inflammation by imaging perivascular fat. Sci Transl Med 2017;9:eaal2658.
24. Oikonomou EK, Marwan M, Desai MY, Mancio J, Alashi A, Hutt Centeno E, et al. Non-invasive detection of coronary inflammation using computed tomography and prediction of residual cardiovascular risk (the CRISP CT study): a post-hoc analysis of prospective outcome data. Lancet 2018;392:929-39.
25. Miyagi M, Ishii H, Murakami R, Isobe S, Hayashi M, Amano T, Arai K, Yoshikawa D, Ohashi T, Uetani T, Yasuda Y, Matsuo S, Matsubara T, Murohara T. Impact of renal function on coronary plaque composition. Nephrol Dial Transplant 2010;25:175-81.
26. Sung J, Chang JH, Chung WJ, Jung JY, Na SY, Lee HH, Sung YM, Moon CI, Hwang YH, Chung W, Kim S. Association between renal dysfunction and the mixed plaque of coronary artery on computed tomographic angiography. Tohoku J Exp Med 2011;225:171-7.
27. Kawai H, Sarai M, Motoyama S, Harigaya H, Ito H, Sanda Y, Biswas S, Anno H, Ishii J, Murohara T, Ozaki Y. Coronary plaque characteristics in patients with mild chronic kidney disease. Analysis by 320-row area detector computed tomography. Circ J 2012;76:1436-41.
28. Kono K, Fujii H, Nakai K, Goto S, Shite J, Hirata K, Fukagawa M, Nishi S. Composition and plaque patterns of coronary culprit lesions and clinical characteristics of patients with chronic kidney disease. Kidney Int 2012;82:344-51.
29. Zoccali C, Mallamaci F, Adamczak M, de Oliveira RB, Massy ZA, Sarafidis P, Agarwal R, Mark PB, Kotanko P, Ferro CJ, Wanner C, Burnier M, Vanholder R, Wiecek A. Cardiovascular complications in chronic kidney disease: a review from the European Renal and Cardiovascular Medicine Working Group of the European Renal Association. Cardiovasc Res 2023;119:2017-32.
30. Shin S, Kim KJ, Chang HJ, Cho I, Kim YJ, Choi BW, Rhee Y, Lim SK, Yang WI, Shim CY, Ha JW, Jang Y, Chung N. Impact of serum calcium and phosphate on coronary atherosclerosis detected by cardiac computed tomography. Eur Heart J 2012;33:2873-81.
31. Huang AL, Leipsic JA, Zekry SB, Sellers S, Ahmadi AA, Blanke P, et al. Effects of chronic kidney disease and declining renal function on coronary atherosclerotic plaque progression: a PARADIGM substudy. Eur Heart J Cardiovasc Imaging 2021;22:1072-82.
32. Li B, Ma L, Jin M, Huang X, Chen M. Left ventricular diastolic dysfunction in uremia patients: the role of four-dimensional automatic left atrial quantification in prediction. Quant Imaging Med Surg 2025;15:12055-68.

Cite this article as: Yuan NL, Zhu WH, Yin WH, Zhu R, An YQ, Hou ZH, Lu B. Quantitative coronary plaque characteristics on coronary computed tomography angiography and their prognostic value in patients with chronic kidney disease. Quant Imaging Med Surg 2026;16(11):844. doi: 10.21037/qims-2026-1-0396